doi.org/10.36721/PJPS.2026.39.7.206.1

Biological synthesis of silver nanoparticles using extracts from *Citrullus colocynthis* and their anticancer activity

Nehad S Alsubhi
Department of Biological Sciences, College of Science, University of Jeddah, Jeddah, Saudi Arabia

Abstract: **Background**: Green synthesis of silver nanoparticles (AgNPs) using plant extract has emerged as an eco-friendly alternative to conventional chemical methods, offering potential biomedical applications, particularly in cancer therapy. **Objectives**: This study aimed to synthesize AgNPs from extracts of *Citrullus colocynthis* leaves, stems and seeds and to evaluate their cytotoxic effects against selected cancer cell lines. **Methods**: AgNPs were biosynthesized using plant extract and characterized using standard analytic techniques. The cytotoxic activity of the synthesized nanoparticles was assessed against A549, HCT116 and MCF-7 cancer cell lines. **Results**: the biosynthesis of AgNPs demonstrated significant anti-cancer activity, with leaf-derived AgNPs showing the strongest cytotoxic effect. Notably, to our knowledge, this study is the first to evaluate leave-derived AgNPs against A549 cells. **Conclusion**: the findings highlight a novel, targeted and environmentally friendly approach for synthesizing AgNPs with promising anti-cancer potential while eliminating the use of toxic chemical agents.

Keywords: Anticancer activity; Breast cancer; *Citrullus colocynthis*; Colon cancer; Green synthesis; Lung cancer; MTT assay; Silver nanoparticles

Submitted on 22-04-2025 – Revised on 25-07-2025 – Accepted on 26-08-2025

INTRODUCTION

Nanotechnology has brought significant advances across various sectors, including medicine, electronics, energy and the environment (Nikalje, 2015). This field focuses on manipulating materials at the nanoscale, typically between 1 and 100 nanometers. Nanoparticles, a key component of nanotechnology, exhibit unique physicochemical properties due to their high surface-to-volume ratios and quantum effects. These properties make nanoparticles highly versatile and effective in numerous applications, particularly in the biomedical field (Dang and Guan, 2020).

In recent years, silver nanoparticles (AgNPs) have attracted significant attention due to their potent antibacterial, antifungal, antiviral and anticancer properties (Rauwel *et al*., 2015, Sofi *et al*., 2022). AgNPs can be synthesized through chemical, physical, or biological methods (Ejaz *et al*., 2024). The chemical synthesis involves the use of reducing agents and stabilizers, whereas the physical approach relies on techniques such as laser ablation and evaporation-condensation. However, these methods can face challenges related to environmental impact, cost and scalability (Kalynovskyi *et al*., 2023).

As a result, the use of biological methods for synthesizing AgNPs, such as utilizing plant extracts and microorganisms, has gained popularity (Palithya *et al*., 2022). These methods are not only simple and scalable but also offer the advantage of incorporating bioactive compounds that naturally act as reducing and capping agents (Fernandes *et al*., 2023). Green synthesis approaches reduce the use of hazardous chemicals and enhance the biological activity of nanoparticles.

**Corresponding author:* e-mail: 04102763@uj.edu.sa

The synthesis of AgNPs using plant extracts is an environmentally friendly and cost-effective approach. Plant extracts, rich in phytochemicals such as flavonoids and polyphenols, act as reducing agents, converting silver ions (Ag^+) from silver nitrate ($AgNO_3$) into metallic silver (Ag^0) (Fig.1). These compounds also serve as stabilizers, preventing nanoparticle aggregation and controlling their size and shape. Factors such as extract concentration, pH and temperature influence the rate of reduction and the characteristics of the nanoparticles. This green synthesis method is gaining attention for its simplicity and sustainability, offering promising applications in areas like medicine, environmental remediation and nanotechnology (Alharbi *et al*., 2022).

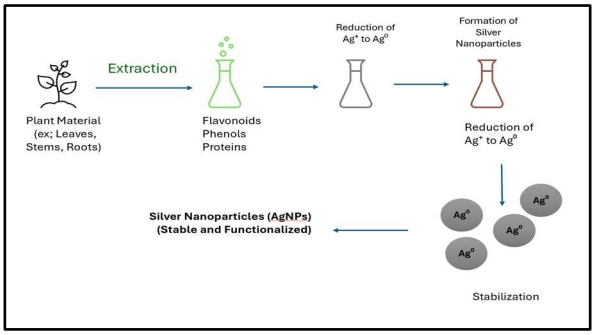

Fig. 1: Schematic diagram of the biosynthesis of AgNPs from plant extracts.

Among the plants explored for the green synthesis of AgNPs is *Citrullus colocynthis*, commonly known as bitter apple or desert gourd (Rao and Poonia, 2023). This plant, which thrives in arid and semi-arid regions, is known for its rich phytochemical profile, including flavonoids, alkaloids and phenolic compounds. In traditional medicine, various parts of *Citrullus colocynthis*, such

as its leaves, fruits, seeds and stems, have been used to treat infections, inflammation and cancer (Sharma and Jain, 2022).

Recent studies have explored the potential of *Citrullus colocynthis* in the green synthesis of AgNPs, utilizing its bioactive compounds for nanoparticle reduction and stabilization (Rasool *et al*., 2022, Samawi *et al*., 2024). These biosynthesized AgNPs have shown promise in the treatment of various cancers, including breast, colon and lung cancers (Rasool *et al*., 2022). Both *Citrullus colocynthis* and AgNPs exhibit synergistic anticancer effects, making them an exciting new option for cancer therapies.

This study focuses on the synthesis of AgNPs from the leaves, seeds and stems of *Citrullus colocynthis* (Fig. 2) and the evaluation of their anticancer potential against breast (MCF-7), colon (HCT116) and lung (A549) cancer cell lines. This is the first report using stem-derived AgNPs against MCF-7 and leaf- and seed-derived AgNPs against A549 cells. The integration of nanotechnology with plant synthesis under different light conditions offers a novel, sustainable and targeted approach for cancer therapy.

Fig. 2: Image of *Citrullus colocynthis* plant

For the extraction process, 5 g of each powdered plant part (leaf, seeds and stems) were separately mixed with 100 mL of deionized water in a beaker. The mixtures were heated to 100°C for 10 min. After heating, the mixtures were allowed to cool to room temperature. The liquid extracts were filtered through Whatman filter paper to separate the solid residues (Khan *et al*., 2023). Fig. 3 illustrates the powdered plant parts and their extraction.

MATERIALS AND METHODS

Water extraction of leaves, seeds and stems of Citrullus colocynthis

Fresh plant materials, including the leaves, seeds and stems of *Citrullus colocynthis*, were collected from desert areas in the Makkah region of Saudi Arabia (Fig. 2). The plant was identified and authenticated by a local botanist. After collection, the plant parts were thoroughly washed with distilled water to remove dirt and debris. The washed samples were air-dried in the shade until constant weight was reached. Once dried, the plant parts were ground into a fine powder using a mortar and pestle to increase the surface area for extraction (Alsubhi, 2024) (Fig. 3).

Fig. 3: Image of the powdered forms of *Citrullus colocynthis* plant parts (leaves, stems and seeds) placed in separate containers (lower row), along with their corresponding aqueous extracts after filtration (upper row), prepared for the green synthesis of AgNPs.

The final concentrated extracts of leaves, seeds and stems were stored separately in tightly sealed glass containers at 4°C for further use.

Phytochemical analysis of plant extracts

Phytochemicals in the extracts of leaves, stems and seeds were identified through qualitative analysis. The presence of flavonoids was confirmed by adding a 10% lead acetate ($Pb(CH_3COO)_2$) solution to the extracts, which resulted in a yellow coloration. Similarly, phenols were detected by introducing a 10% ferric chloride ($FeCl_3$) solution, leading to a bluish-black color change (Kalynovskyi *et al*., 2023). The Salkowski and gelatin tests were used to detect tannins; the formation of sediments indicated their presence. The distinct color changes observed further validated the presence of these phytochemicals.

Biosynthesis of silver nanoparticles

Silver nanoparticles were synthesized by mixing 1 mL of *Citrullus colocynthis* extract with 1 mM $AgNO_3$ solution. The formation of AgNPs was tested under three distinct conditions to evaluate optimal synthesis parameters: (1) under direct sunlight for 5 minutes, with an ambient temperature of approximately 30 °C (The sunlight exposure time was selected based on preliminary

optimization experiments, during which a color change was observed to stabilize after 5 minutes, indicating the completion of the nanoparticle formation process), (2) at room temperature (25 °C) under standard indoor lighting conditions (~300-500 lux) and (3) in complete darkness at room temperature. These variations were designed to assess the effects of light intensity and temperature on nanoparticle formation, ensuring reproducibility by maintaining controlled and documented environmental conditions.

Characterization of silver nanoparticles using UV-Vis spectroscopy, SEM and FTIR

UV-Vis Spectroscopy: The formation of AgNPs was first evaluated using UV-Vis spectroscopy. A small portion of the synthesized nanoparticle solution was placed in a glass cuvette. The absorption spectrum was recorded over 300-600 nm, focusing on the surface plasmon resonance (SPR) peak, which typically appears at 400-500 nm for AgNPs. The position and intensity of the SPR band provided crucial information regarding the particle size, shape and efficiency of nanoparticle synthesis, as well as the stability of the nanoparticles (Kitimu *et al*., 2022).

Fourier transform infrared spectroscopy (FTIR): To identify the bioactive compounds involved in the reduction and stabilization of the AgNPs, Fourier Transform Infrared (FTIR) spectroscopy (model no: NICOLET iS10, Thermo Fisher Scientific, Waltham, MA, USA) was performed. The dried AgNPs powder was mixed with potassium bromide (KBr) to form a pellet and the FTIR spectrum was recorded between 4000 and 600 cm^{-1}. The observed peaks indicated the presence of functional groups from the plant extract, which likely played a role in the reduction of Ag^{+} and stabilization of the nanoparticles (Santhoshkumar *et al*., 2021).

Field Emission Scanning electron microscopy (SEM): Scanning Electron Microscopy (FESEM) (model Jeol 7600 F FESEM, Tokyo, Japan) was utilized to observe the morphology and size of the AgNPs. A drop of the nanoparticle solution was placed onto an SEM stub and allowed to air-dry. The sample was then gold-coated to improve conductivity and imaged at 120,000x using the SEM. SEM provided detailed images of the nanoparticles' size, shape and surface characteristics, which helped confirm their uniformity and dimensions (Alsubhi, 2024).

MTT assay

According to the method of (Felimban *et al*., 2022) The MTT assay was used to evaluate the anticancer activity of AgNPs synthesized from *Citrullus colocynthis* extract against A549 (lung cancer), MCF7 (breast cancer) and HCT116 (colorectal cancer) cell lines. In this experiment, 10,000 cells were plated per well in a 96-well plate and cultured until reaching optimal confluence. The cells were then treated with varying concentrations of AgNPs (6.25, 12.5, 25, 50, 100 and 200 µg/mL). After 48 hours of incubation, MTT solution was added to each well. Active cells reduced the MTT reagent, forming purple formazan crystals. After a 4-hour incubation with the MTT reagent, the formazan crystals were solubilized and absorbance was measured at 570 nm. The reduction in absorbance indicated decreased cell viability, suggesting that AgNPs caused cytotoxicity and inhibited cell proliferation. The results were compared to those of the untreated control group to assess the effectiveness of the nanoparticles. This analysis provided valuable insight into the potential therapeutic applications of AgNPs synthesized from *Citrullus colocynthis* in cancer treatment.

DNA fragmentation assay

The DNA fragmentation assay was conducted to investigate the apoptotic effects of AgNPs synthesized using *Citrullus colocynthis* extracts on A549, MCF7 and HCT116 cancer cell lines. Cells were cultured in standard conditions and treated with IC50 concentrations of AgNPs for 72 hours, with untreated cells serving as controls. After treatment, cells were harvested, washed with phosphate-buffered saline (PBS) and lysed with a buffer containing Tris-HCl, EDTA and SDS. RNA was removed using RNase and protein digestion was carried out with proteinase K. DNA was precipitated with isopropanol, washed with ethanol and resuspended in TE buffer. The purified DNA was analyzed via agarose gel electrophoresis. Fragmented DNA, indicative of apoptosis, displayed a characteristic ladder pattern, while intact DNA appeared as a single high-molecular-weight band. This method successfully demonstrated the pro-apoptotic activity of *Citrullus colocynthis*-derived AgNPs against the cancer cells (Jagatheesh *et al*., 2021).

DAPI staining

DAPI (4′,6-diamidino-2-phenylindole) staining was performed to evaluate apoptosis in A549, MCF7 and HCT116 cancer cells treated with AgNPs synthesized using *Citrullus colocynthis* extracts. Cells were fixed with 4% paraformaldehyde to preserve their structure, then stained with a DAPI solution (1-5 µg/mL) in the dark to prevent fluorescence loss. After incubation, excess DAPI was removed by washing with phosphate-buffered saline (PBS). Stained cells were mounted with an anti-fade medium and examined under a fluorescence microscope (excitation at ~358 nm, emission at ~461 nm) (Baker *et al*., 2021). Apoptotic cells showed bright, condensed, or fragmented nuclei, while intact nuclei appeared uniformly stained and larger. This method effectively demonstrated the apoptotic effects of *Citrullus colocynthis*-derived AgNPs, showcasing their potential as anti-cancer agents.

Cell morphologies

Cell morphology analysis was performed to examine the impact of AgNPs synthesized from *Citrullus colocynthis* extracts on A549, MCF7 and HCT116 cancer cells. The

cells were treated with different concentrations of AgNPs for 72 hours, with untreated cells serving as controls. Following treatment, cells were fixed using 4% paraformaldehyde to maintain structural integrity. Light microscopy, enhanced with crystal violet staining, was used to observe general morphological changes. Fluorescence microscopy with acridine orange and ethidium bromide staining allowed differentiation between viable, apoptotic and necrotic cells (Pannerselvam *et al*., 2021). Apoptotic cells were identified by characteristic features, such as chromatin condensation, nuclear fragmentation and membrane blebbing. These observations highlighted the apoptotic effects of *Citrullus colocynthis*-derived AgNPs, demonstrating their potential as anticancer agents.

Statistical analysis

The results are presented as the average of three independent experimental replicates, including their standard deviations. Graphs were prepared using Microsoft Excel and statistical significance was evaluated through a one-way analysis of variance (ANOVA) performed with SPSS software (SPSS Inc., Chicago, IL, USA). The significance levels were noted as $^{**}p \leq 0.01$, $^{*}p \leq 0.05$ and $^{***}p \leq 0.001$.

RESULTS

Phytochemical analysis of plant extracts

The appearance of a yellow color indicated flavonoids; a bluish-black coloration confirmed the presence of polyphenols and tannins, as evidenced by the formation of precipitates in the extracts. Fig. 4 illustrates the results of the phytochemical analysis, showing the visual confirmation of flavonoids (yellow coloration), polyphenols (bluish-black coloration) and tannins (formation of precipitates) in the plant extracts.

Fig. 4: Visual representation of phytochemical analysis results for flavonoids (yellow coloration), polyphenols (bluish-black coloration) and tannins (formation of precipitates) in leaf, seed and stem extracts.

Biosynthesis of AgNPs

The nanoparticles were successfully synthesized using extracts from the leaves, seeds and stems of *Citrullus colocynthis* under room light, darkness and sunlight. The reaction mixtures displayed distinct color changes, with the most pronounced and rapid changes observed under sunlight (Fig. 5). UV-Vis spectroscopy confirmed the formation of AgNPs, showing surface plasmon resonance (SPR) peaks at 450 nm for the leaf extract, 444 nm for the seed extract and 465 nm for the stem extract under sunlight (Fig. 6). These peaks were narrower and more intense compared to those obtained under room light or darkness, indicating a higher yield and better uniformity of nanoparticles.

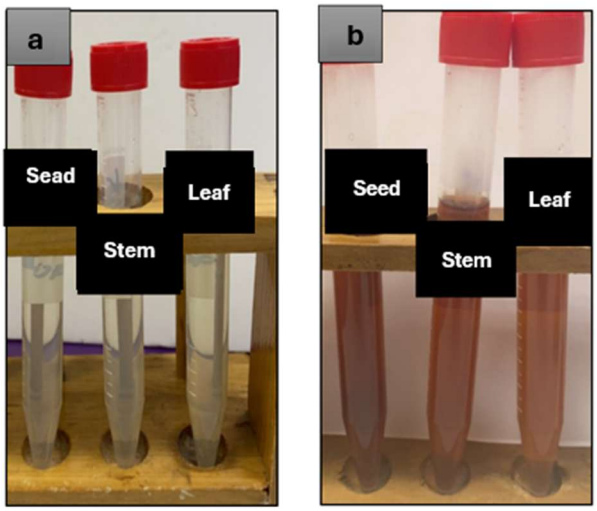

Fig. 5: Visual comparison of AgNo3 solution (a) before synthesis and (b) after bioreduction using aqueous extracts of *Citrullus colocynthis* leaf, seed and stem. The color change indicates the formation of AgNPs.

Characterization of BioAgNPs

FTIR

Fourier Transform Infrared spectroscopy analysis identified functional groups in the *Citrullus colocynthis* extracts that were involved in the biosynthesis of AgNPs. Peaks in the spectra of the extracts were observed at 3200-3600 cm^{-1}, representing O-H stretching vibrations, 1600-1700 cm^{-1} for C=O stretching, 1400 cm^{-1} for C-H bending and 1000-1200 cm^{-1} for C-O stretching. The seed extract also shows a peak at around 2860 cm^{-1} corresponding to the OH group. After AgNP synthesis, these peaks were either significantly reduced or disappeared, indicating that the functional groups were used to reduce Ag^{+} and stabilize the nanoparticles. Fig. 7 illustrates the FTIR spectra of plant extracts and their biosynthesized AgNPs.

SEM

The Scanning Electron Microscopy analysis at 120,000x magnification confirmed the successful biosynthesis of AgNPs using *Citrullus colocynthis* extracts. The nanoparticles exhibited spherical and ribbed shapes, with average sizes measured at 24 nm for the leaf extract, 31 nm for the stem extract and 30 nm for the seed extract (Fig. 8). Minor agglomeration was observed, though the nanoparticles generally maintained a consistent size range for all extracts.

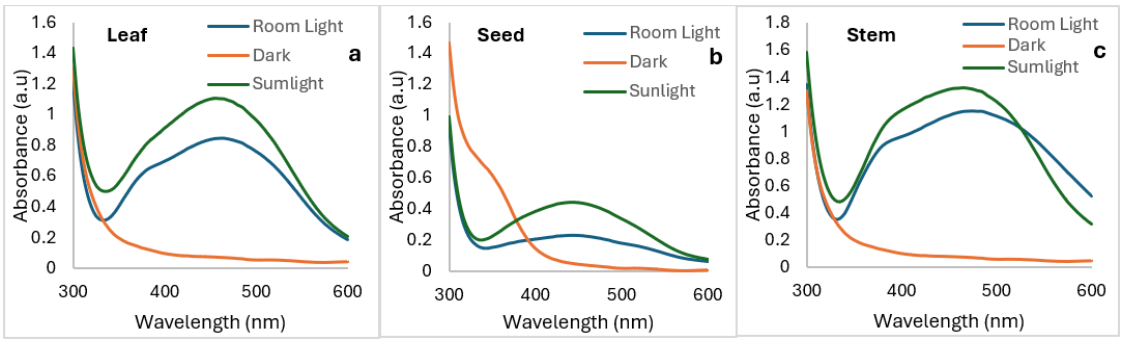

Fig. 6: UV-Vis spectra of *Citrullus colocynthis* extracts under different light conditions. (a) leaf extract, (b) seed extract and (c) stem extract. Each subfigure shows the observation spectra recorded under three conditions: room light, sunlight and darkness. Absorbance was measured over the wavelength range of 300- 600 nm.

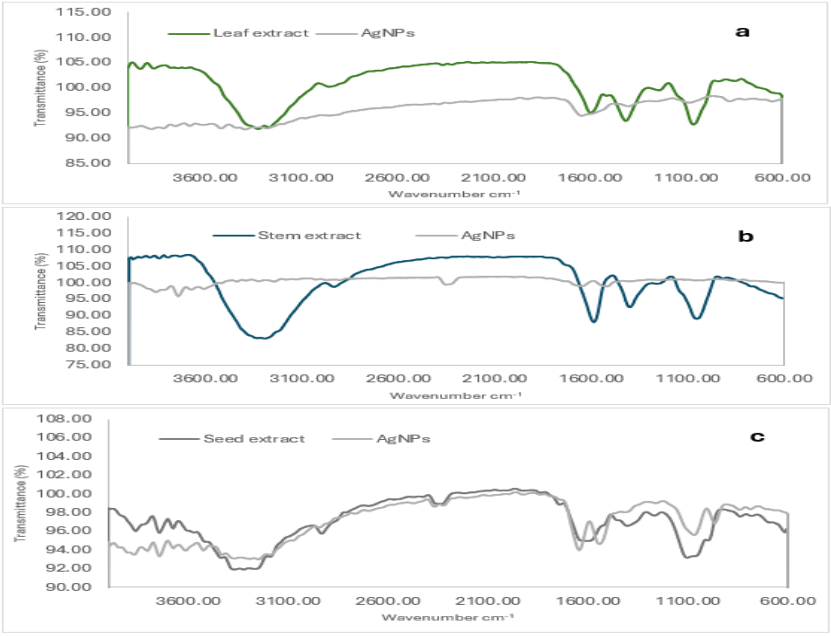

Fig. 7: FTIR Spectra of *Citrullus colocynthis* plant extracts and their synthesized silver nanoparticles (AgNPs). (a) leaf derived AgNPs; (b) stem derived AgNPs and; (c) seed derived AgNPs. The spectra were recorded in the range of 600-3600 cm-1 to identify the functional group responsible for the reduction and stabilization of AgNPs.

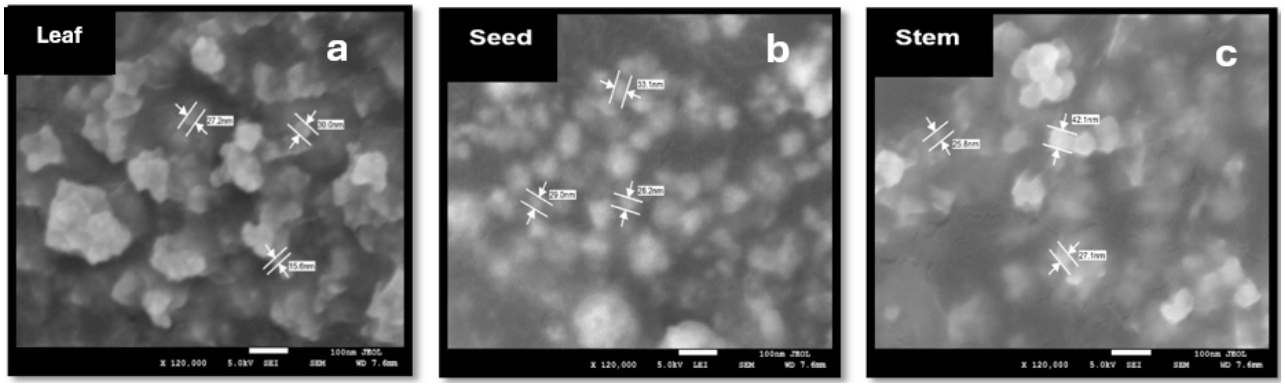

Fig. 8: FESEM images of AgNPs biosynthesized using *Citrullus colocynthis* plant extracts, captured at a magnification of 120,000×. (a) leaf derived AgNPs; (b) seed derived AgNPs and; (c) stem derived AgNPs. The images reveal the morphology and surface characteristics of the synthesized nanoparticles.

The characterization results indicated that AgNPs synthesized from the leaf extract demonstrated exceptional quality. Therefore, the MTT assay was conducted to evaluate the cytotoxic effects of these nanoparticles against breast, colon, and lung cancer cell lines.

MTT assay

The MTT assay results demonstrated the cytotoxic effects of AgNPs synthesized using *Citrullus colocynthis* leaf extracts on different cancer cell lines (Fig. 9). The half-maximal inhibitory concentration (IC50) values revealed varying levels of sensitivity among the tested cell lines. The IC50 value for MCF7 cells was 116.6 µg/mL, indicating moderate sensitivity. HCT116 cells showed the highest sensitivity to AgNPs, with an IC50 value of 62.71 µg/mL. In comparison, A549 cells exhibited the lowest sensitivity, with an IC50 value of 122.8 µg/mL. These results confirm the differential cytotoxic effects of AgNPs on the tested cancer cell lines.

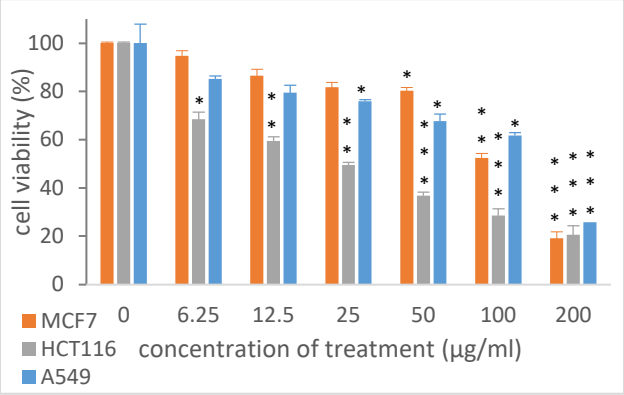

Fig. 9: The cytotoxic potential of bioAgNPs, derived via green synthesis from *Citrullus colocynthis* leaf extracts, was evaluated against A549, HCT116 and MCF-7 cancer cell lines using the MTT assay. Triplicate experiments were conducted to ensure reproducibility and results were expressed as mean values ± standard deviation (SD). Statistical analysis was performed using one-way ANOVA followed by Tukey's post hoc test to assess intergroup differences. Significance levels were indicated as follows: $^{*}P \leq 0.05$, $^{**}P \leq 0.01$ and $^{***}P \leq 0.001$. All statistical evaluations were conducted using SPSS software, version 28.0 (SPSS Inc., Chicago, IL, USA).

DNA fragmentation

The results of the DNA fragmentation assay (Fig. 10) showed clear evidence of DNA damage in A549, MCF7 and HCT116 cells treated with AgNPs synthesized using *Citrullus colocynthis* leaf extract at IC50 concentrations. Gel electrophoresis revealed intact, high-molecular-weight DNA bands in untreated control cells, whereas cells treated with AgNPs displayed smeared DNA patterns, indicating fragmentation.

DAPI staining

DAPI staining results revealed nuclear alterations in A549, MCF7 and HCT116 cells treated with AgNPs synthesized from *Citrullus colocynthis* leaf extract at IC50 concentrations. Fluorescence microscopy showed intact, uniformly stained nuclei in control cells. In contrast, AgNP-treated cells displayed condensed and fragmented nuclei in all cell lines (Fig. 11)

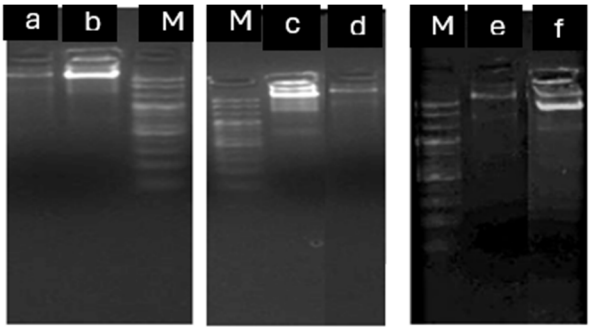

Fig. 10: Gel electrophoresis analysis of DNA from treated and untreated cell lines. (M) DNA marker, (a) A549 untreated cells, (b) A549 cells treated with AgNPs biosynthesized from leaf extract, (c) MCF7 cells treated with AgNPs biosynthesized from leaf extract, (d) MCF7 untreated cells, (e) HCT116 untreated cells and (f) HCT116 cells treated with AgNPs biosynthesized from leaf extract. DNA fragmentation patterns were analyzed to evaluate apoptosis induction.

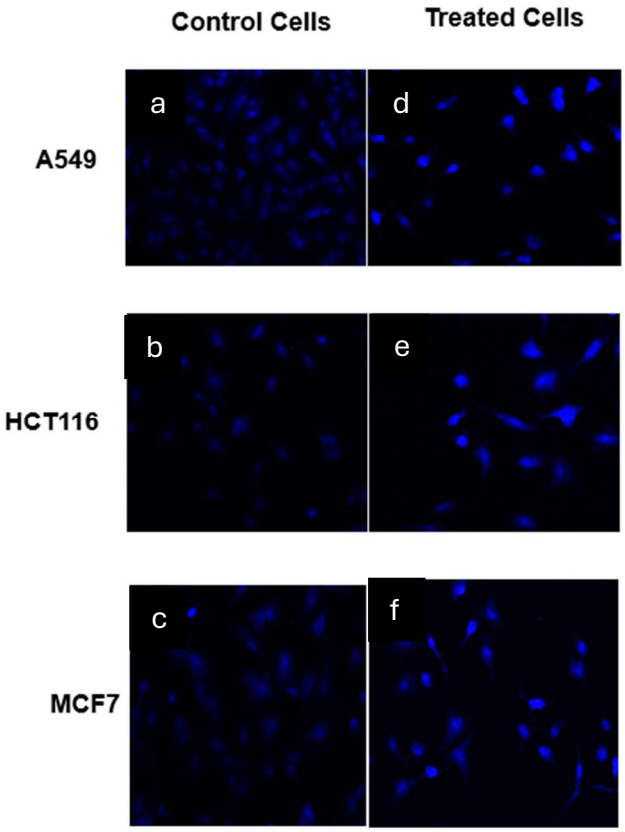

Fig. 11: Fluorescence microscopy images of DAPI stained. (a, b, c) Control (untreated) and (d, e, f) AgNPs treated cell lines. Subfigures represent different cell types under control and treatment conditions. DAPI staining was used to evaluate nuclear morphology and detect apoptotic changes. The treated cells (A549, HCT116 and MCF7) exhibit nuclear condensation and fragmentation compared to their respective untreated cells, indicating apoptosis

induction following exposure to AgNPs biosynthesized from leaf extract.

Cell morphologies

The cell morphology results, as shown in fig. 12, indicated noticeable changes in A549, MCF7 and HCT116 cells treated with AgNPs synthesized from *Citrullus colocynthis* leaf extract at IC50 concentrations. Untreated control cells maintained normal morphology with intact, uniform cell shapes. In contrast, treated cells exhibited significant morphological alterations, such as cell shrinkage, membrane blebbing and irregular shapes, all hallmarks of apoptosis.

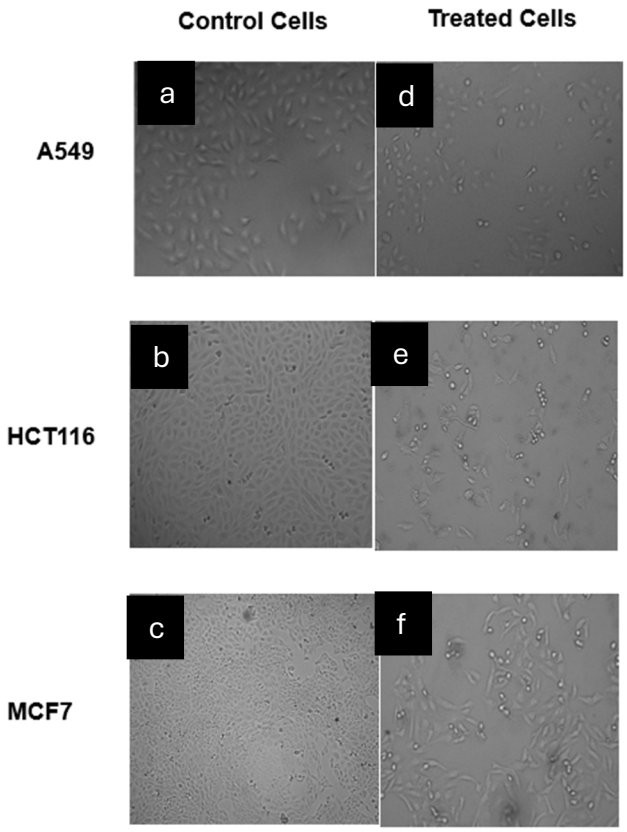

Fig. 12: Morphological analysis of A549, HCT116 and MCF-7 cancer cell lines after 24 hours of treatment with biosynthesized AgNPs. (a, b, c) Control (untreated) cells display normal morphology, with a flattened and spread appearance. In contrast, (d, e, f) AgNP-treated cells exhibit marked apoptotic features, including cell shrinkage, rounding, detachment from the culture surface and overall loss of structural integrity, indicating a significant cytotoxic effect induced by the nanoparticles.

DISCUSSION

The biosynthesis of AgNPs from *Citrullus colocynthis* leaf, seed and stem extracts demonstrated distinct variations in the properties and effectiveness of the nanoparticles produced, with the leaf extract yielding the highest quality AgNPs. This is consistent with findings from previous studies where plant extracts rich in phenolic compounds, flavonoids and alkaloids played a significant role in the reduction and stabilization of Ag^{+} into nanoparticles (Rasool *et al*., 2022). The sharp and intense surface plasmon resonance (SPR) peaks observed under sunlight for AgNPs synthesized from leaf extracts further indicated efficient nanoparticle formation and a narrow size distribution. This could be attributed to the phytochemicals present in the leaf extract, which acted as reducing agents and stabilizers during nanoparticle formation (Alsubhi, 2024).

The cytotoxicity results from the MTT assay revealed that AgNPs synthesized from the leaf extract exhibited potent anticancer effects, with the lowest IC50 value against HCT116 cells (62.71 µg/mL), which were more sensitive to nanoparticles compared to MCF7 and A549 cells. This finding aligns with reports that AgNPs can exhibit selective toxicity against various cancer cell lines, possibly due to variation in cellular uptake and interactions with cellular components (Hou *et al*., 2023). In this study, MCF7 cells showed moderate sensitivity (IC50 = 116.6 µg/mL), while A549 cells exhibited the least sensitivity (IC50 = 122.8 µg/mL), which may be attributed to inherent differences in the mechanisms of drug resistance or nanoparticle uptake in these cell lines (Alsubhi, 2024).

The DNA fragmentation test provided initial evidence of cytotoxic effects of AgNPs, as DNA smearing was observed in the treated cells, particularly in the HCT116 line. While DNA fragmentation is often associated with apoptosis, the smeared pattern could also indicate necrotic processes. Without further molecular validation, the exact nature of cell death therefore remains uncertain. These findings are consistent with previous studies reporting AgNP-induced genotoxicity in cancer cells (Ponmani *et al*., 2021, Ramachandran *et al*., 2022). In addition, DAPI staining revealed nuclear condensation and fragmentation, suggesting apoptotic events. A similar study demonstrated that DAPI staining assays revealed that AgNPs biosynthesized from leaf extracts exhibit greater cytotoxicity against lung cancer cell lines (Alsubhi *et al*., 2024)

However, in the absence of confirmatory assays such as caspase activity or ROS quantification, these interpretations should be considered preliminary.

In addition, the cell morphology analysis revealed clear signs of apoptosis, such as cell shrinkage, membrane blebbing and irregular shapes, (Ghose *et al*., 2022). The more pronounced changes observed in HCT116 cells further validate the selective cytotoxicity of AgNPs.

Mechanisms of AgNPs on cancer cells

The anticancer effects of AgNPs have been attributed to multiple mechanisms, including reactive oxygen species

(ROS) generation, mitochondrial dysfunction, DNA damage and apoptosis induction. One of the primary mechanisms of AgNP-induced cytotoxicity is the excessive generation of ROS, which leads to oxidative stress, lipid peroxidation and cellular damage (Rohde *et al*., 2021). Increased ROS levels disrupt mitochondrial membrane potential, causing cytochrome c release and activation of the caspase cascade, ultimately leading to apoptosis (Zaib *et al*., 2022).

Additionally, AgNPs interact with cellular proteins and DNA, leading to genotoxic effects. The nanoparticles penetrate the nucleus, causing DNA strand breaks and chromosomal instability, which can trigger apoptosis (Chen *et al*., 2024). The DNA fragmentation results from this study further support this mechanism. Moreover, AgNPs disrupt cellular signaling pathways by interfering with kinase activities and suppressing tumor-promoting factors such as NF-κB, leading to cancer cell death (Xiong *et al*., 2025).

Furthermore, AgNPs induce apoptosis via both intrinsic and extrinsic pathways. The intrinsic pathway is mediated by mitochondrial damage, while the extrinsic pathway involves death receptor activation, such as Fas/FasL and TNF-related apoptosis-inducing ligand (TRAIL), leading to caspase-dependent apoptosis (Chaudhary *et al*., 2024). The ability of AgNPs to selectively target cancer cells while sparing normal cells is attributed to differences in oxidative stress response and nanoparticle uptake between malignant and non-malignant cells (Kumarasamy *et al*., 2025).

CONCLUSION

This study demonstrated the green synthesis of AgNPs using leaves, stems and seeds of *Citrullus colocynthis*, with characterization confirming successful nanoparticle formation. The biosynthesized AgNPs exhibited notable cytotoxic effects against breast (MCF-7), colon (HCT116) and lung (A549) cancer cell lines, particularly those derived from leaves and stems. While the IC_{50} values suggest moderate activity, these findings indicate a potential therapeutic role that warrants further investigation, particularly studies including normal cell lines to assess selectivity. The synthesis approach employed in this work used environmentally benign conditions without hazardous chemicals, aligning with green chemistry principles, though no formal environmental impact assessment was conducted. Overall, this study contributes novel insights into the anticancer potential of *Citrullus colocynthis*-mediated AgNPs and highlights key areas for future research, including mechanistic studies and *in-vivo* validation.

Acknowledgements
Not applicable

Author's contributions
The author solely conceived, designed, conducted, analyzed and wrote this study.

Funding
There was no funding.

Data availability statement
All data generated or analyzed during this study are included in this published article [and its supplementary information files].

Ethical approval
Not applicable.

Conflicts of interest
The authors declare that they have no conflicts of interest related to this work.

REFERENCES

Alharbi NS, Alsubhi NS and Felimban AI (2022). Green synthesis of nanoparticles using medicinal plants: Characterization and application. *J. Radiat. Res. Appl. Sci.,* **15**(3): 109-124.

Alsubhi NS (2024). Biological synthesis of silver nanoparticles from *Juniperus procera* and *Azadirachta indica* stem extracts and their anticancer properties. *J. Biomed. Nanotechnol.,* **20**(11): 1736-1746.

Baker A, Iram S, Syed A, Elgorban AM, Bahkali AH, Ahmad K, Sajid Khan M and Kim J (2021). Fruit derived potentially bioactive bioengineered silver nanoparticles. *Int. J. Nanomed.,* 7711-7726.

Chaudhary P, Janmeda P, Pareek A, Chuturgoon AA, Sharma R and Pareek A (2024). Etiology of lung carcinoma and treatment through medicinal plants, marine plants and green synthesized nanoparticles: A comprehensive review. *Biomed. Pharmacother.,* **173**: 116294.

Chen Q, Fang C, Xia F, Wang Q, Li F and Ling D (2024). Metal nanoparticles for cancer therapy: Precision targeting of DNA damage. *Acta Pharm. Sin. B.,* **14**(3): 1132-1149.

Dang Y and Guan J (2020). Nanoparticle-based drug delivery systems for cancer therapy. *Smart Mater. Med.,* **1**: 10-19.

Ejaz U, Afzal M, Mazhar M, Riaz M, Ahmed N, Rizg WY, Alahmadi AA, Badr MY, Mushtaq RY and Yean CY (2024). Characterization, synthesis and biological activities of silver nanoparticles produced via green synthesis method using *Thymus vulgaris* aqueous extract. *Int. J. Nanomed.,* 453-469.

Felimban AI, Alharbi NS and Alsubhi NS (2022). Optimization, characterization and anticancer potential of silver nanoparticles biosynthesized using Olea europaea. *Int. J. Biomater.,* **2022**: 6859637.

Fernandes C, Jathar M, Sawant BKS and Warde T (2023). Scale-up of nanoparticle manufacturing process. *Pharm. Process Eng. Scale-up Principles. Springer.,* 173-203.

Ghose R, Asaduzzaman A, Hasan I and Kabir SR (2022). *Hypnea musciformis*-mediated Ag/AgCl-NPs inhibit pathogenic bacteria, HCT-116 and MCF-7 cells' growth *in-vitro* and Ehrlich ascites carcinoma cells *in-vivo* in mice. *IET Nanobiotechnol.,* **16**(2): 49-60.

Hou T, Guo Y, Han W, Zhou Y, Netala VR, Li H, Li H and Zhang Z (2023). Exploring the biomedical applications of biosynthesized silver nanoparticles using Perilla frutescens flavonoid extract: Antibacterial, antioxidant and cell toxicity properties against colon cancer cells. *Molecules,* **28** (17): 6431.

Jagatheesh S, Anandhi D and Revathi K (2021) Phytochemical and cytotoxic effects of silver nanoparticles synthesized from *Chromolaena odorata* plant on MG-63 Cell line. *Int. J. Pharm. Res.,* **13**(3): 1804-1809.

Kalynovskyi V, Smirnov O, Zelena P, Yumyna Y, Kovalenko M, Dzhagan V, Dzerzhynsky M and Taran N (2023). Biosynthesis of silver nanoparticles with antioxidant and bactericidal activities using *Capsicum annuum* fruit extract. Regul. *Mech. Biosyst.,* **14**(3): 393-398.

Khan M, Khan T, Wahab S, Aasim M, Sherazi TA, Zahoor M and Yun SI (2023). Solvent based fractional biosynthesis, phytochemical analysis and biological activity of silver nanoparticles obtained from the extract of *Salvia moorcroftiana*. *PLoS One,* **18**(10): e0287080.

Kitimu SR, Kirira P, Sokei J, Ochwangi D, Mwitari P and Maina N (2022). Biogenic synthesis of silver nanoparticles using *Azadirachta indica* methanolic bark extract and their anti-proliferative activities against DU-145 human prostate cancer cells. *Afr. J. Biotechnol.,* **21**(2): 64-72.

Kumarasamy RV, Natarajan, PM, Mathivanan I, Balasubramaniam M, SN S, Prabhu D, Raju K, Mironescu M and Mironescu ID (2025). Sustainable biogenic synthesis of silver nanoparticles for oral cancer: A comprehensive review. *Frontiers in Nanotechnology*, **7**: 1648900.

Nikalje AP (2015). Nanotechnology and its applications in medicine. *Med. Chem.,* **5**(2): 081-089.

Palithya S, Gaddam SA, Kotakadi VS, Penchalaneni J, Golla N, Krishna SBN and Naidu C (2022). Green synthesis of silver nanoparticles using flower extracts of Aerva lanata and their biomedical applications. *Particulate Sci. Technol.,* **40**(1): 84-96.

Pannerselvam B, Thiyagarajan D, Pazhani A, Thangavelu KP, Kim HJ and Rangarajulu SK (2021). Copperpod plant synthesized AgNPs enhance cytotoxic and apoptotic effect in cancer cell lines. *Processes,* **9**(5): 888.

Ponmani J, Kanakarajan S, Selvaraj R and Kamalanathan A (2021). Induced apoptotic potential of green synthesized AgNPs from *Sargassum wightii* on human prostate cancer (PC-3) cells. *Chettinad Health City Med. J.,* **10**: 127-135.

Ramachandran R, Parthasarathy R and Dhayalan S (2022). Silver nanoparticles synthesized by *Euphorbia hirta* exhibited antibacterial activity and induced apoptosis through downregulation of PI3Kγ mediated PI3K/Akt/mTOR/p70S6K in human lung adenocarcinoma A549 cells. *Environ. Toxicol.,* **37**(12): 2865-2876.

Rao V and Poonia A (2023). *Citrullus colocynthis* (bitter apple): Bioactive compounds, nutritional profile, nutraceutical properties and potential food applications: A review. *Food Prod. Process. Nutr.,* **5**(1): 4.

Rasool S, Tayyeb A, Raza MA, Ashfaq H, Perveen S, Kanwal Z, Riaz S, Naseem S, Abbas N and Ahmad N (2022). *Citrullus colocynthis*-mediated green synthesis of silver nanoparticles and their antiproliferative action against breast cancer cells and bactericidal roles against human pathogens. *Nanomaterials,* **12**(21): 3781.

Rauwel P, Rauwel E, Ferdov S and Singh MP (2015). Silver nanoparticles: Synthesis, properties and applications. *Adv. Mater. Sci. Eng.,* **2015**(2): 1-2.

Rohde MM, Snyder CM, Sloop J, Solst SR, Donati GL, Spitz DR, Furdui CM and Singh R (2021). The mechanism of cell death induced by silver nanoparticles is distinct from silver cations. *Particle Fibre Toxicol.,* **18**(1): 1-24.

Samawi MK, Alsalihy AA and Suleiman A (2024). Use of *Citrullus colocynthis* callus for green synthesis of silver nanoparticles and their activity against biofilm-producing. *J. Commun. Dis.,* **56**(2): 94-99.

Santhoshkumar R, Hima Parvathy A and Soniya E (2021). Phytosynthesis of silver nanoparticles from aqueous leaf extracts of *Piper colubrinum*: Characterisation and catalytic activity. *J. Exp. Nanosci.,* **16**(1): 294-308.

Sharma DK and Jain VK (2022). Therapeutic, ethnomedicinal and pharmacological perspective of bitter apple fruit (*Citrullus colocynthis* (L.) Schrad.). *Cent. Asian J. Med. Nat. Sci.,* **3**(4): 260-267.

Sofi MA, Sunitha S, Sofi MA, Pasha SK and Choi D (2022). An overview of antimicrobial and anticancer potential of silver nanoparticles. *J. King Saud Univ. Sci.,* **34**(2): 101791.

Xiong Z, Huang Y, Cao S, Huang X and Zhang H (2025). A new strategy for the treatment of advanced ovarian cancer: utilizing nanotechnology to regulate the tumor microenvironment. *Front. Immunol*., **16**: 1542326.

Zaib S, Hayyat A, Ali N, Gul A, Naveed M and Khan I (2022). Role of mitochondrial membrane potential and lactate dehydrogenase A in apoptosis. *Anticancer Agents Med. Chem.,* **22**: 2048-2062.